Check for updates

Physical organic studies and dynamic covalent chemistry of picolyl heterocyclic amino aminals†

Ji-Ming Ciou,[a] Hong-Feng Zhu,[b] Chia-Wen Chang,[a] Jing-Yun Chen[a] and Ya-Fan Lin [ID] *[ab]

A dynamic covalent system of the picolyl heterocyclic amino aminals has been studied. The aminals are characterized as a metastable species and easily switch to other forms *via* external stimuli. The solvent, temperature, acid–base and substituent effects have been examined to evaluate the dynamic covalent system. The results reveal that a more polar solvent, a lower temperature, basic conditions and an electron-withdrawing moiety contribute to the stabilities of aminals. The existence of the n → π* interaction between acetonitrile and the C=N moiety makes the *N*-pyrimidyl imine (**4c** and **4d**) yield higher in CD_3CN. In a similar fashion, all aminals tend to convert to the corresponding hemiaminal ethers in a methanol environment. According to these findings, we successfully synthesized the following species: (a) *N*-2-picolylpyrimidin-2-amine **6c** obtained by reduction using acetonitrile as the specific solvent; (b) a picolyl aromatic amino aminal **3e** prepared from 2-pyridinecarboxaldehyde and the electron withdrawing 2-methoxy-5-nitroaniline.

Introduction

Dynamic covalent chemistry is defined as a covalent bond that forms or breaks reversibly.[1–7] Several components undergo continuous exchange and reach an equilibrium in a stable distribution.[8–11] A dynamic covalent system can respond to external stimuli to achieve adaption, bringing dynamic diversity to allow variation and selection.[12–17] As a result, if the transition of the different states can be controlled *via* external stimuli, the chemical system can be considered as a kind of molecular switch.[18–21] Imine is one of the known dynamic covalent systems, which have been widely utilized in several fields, such as many enzymatic processes and development of dynamic materials.[22–26] Although dynamic imine formation processes are known to include several reversible reactions such as hydrolysis,[27] transimination[28–32] and imine metathesis,[33–35] limited studies have reported the observation and isolation of the corresponding intermediates such as aminals, hemiaminals and hemiaminal ethers.[36–45] To develop new functions by understanding the thermodynamic and bonding properties, there is still a great demanding to explore suitable systems which can be successfully detected intermediates.

[a]Department of Fragrance and Cosmetic Science, Kaohsiung Medical University, 100 Shi-Chuan 1st Rd., San-Ming Dist., Kaohsiung, 80708, Taiwan. E-mail: yafan@kmu.edu.tw

[b]Department of Medicinal and Applied Chemistry, Kaohsiung Medical University, Kaohsiung 80708, Taiwan

† Electronic supplementary information (ESI) available. CCDC 1961718–1961721. For ESI and crystallographic data in CIF or other electronic format see DOI: 10.1039/d0ra08527h

Herein, we re-examined the physical organic properties and the dynamic covalent chemistry (DCC) of a series of picolyl heterocyclic amino aminals.[46] Although the synthesis and characterization of this system have been reported,[47] the dynamic behaviours such as the equilibria between aminals and the corresponding imines remain unclear. To explore the molecular properties of aminals more deeply, we decided to investigate the responsiveness of this system to the external stimuli such as solvent, acid–base, substituent and temperature effect. It was found that the entity of the heterocyclic amine would be predominant to the molecular behaviours. Furthermore, since the switch of the equilibrating states in this system can be well-controlled by an environmental stimulus, we therefore presented aminal reduction and the synthesis of a novel picolyl aromatic amino aminal in accordance with the different tuning factors.

Results and discussion
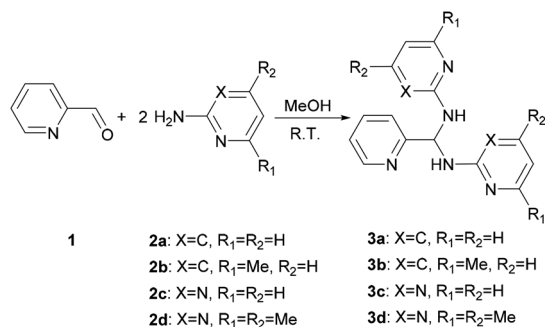
Synthesis of picolyl heterocyclic amino aminals

Treatment of a methanol solution of 2-pyridinecarboxaldehyde (**1**) with 2 equivalent of 2-amino-heterocyclic **2a–d** at room temperature (301 K) gives **3a–d** (Scheme 1). Changing the reactant ratio only varies the yields but not the products. For the solid state characterization, elemental analysis of **3a–d** agrees with the aminal formulas (Table 1). Single crystal diffraction analysis reveals **3a** and **3c** crystallize as an aminal structure with space groups of *Pbcn* and *P*21/*n*, respectively (Fig. S1†). All structural parameters show similar values to the literature data.[48]

Scheme 1 Synthesis route for **3a–d**.

Table 1 Elemental analysis of aminals **3a–d**

No.	Formula	Calculated, %			Found, %		
		C	H	N	C	H	N
3a	$C_{16}H_{15}N_5$	69.29	5.45	25.25	69.15	5.43	25.29
3b	$C_{18}H_{19}N_5$	70.80	6.27	22.93	70.76	6.28	23.06
3c	$C_{14}H_{13}N_7$	60.20	4.69	35.10	60.16	4.73	35.37
3d	$C_{18}H_{21}N_7$	64.46	6.31	29.23	64.20	6.25	29.36

Interestingly, the molecular structures of **3c** and **3d** in solution are consistent with those characterized in solid state, whilst it shows an imine-aminal equilibrium when **3a** and **3b** are dissolved in CDCl₃ (Scheme 2). The ¹H NMR spectra of **3c** and **3d** in CDCl₃ reveal no peak at the typical imine regions (7.7–9.5 ppm). Meanwhile, a triplet around 7.1 ppm attributed to the methine (–CH–) group was observed in both cases of **3c** and **3d**. In contrast, when **3a** and **3b** were dissolved in CDCl₃, the ¹H NMR spectra showed two sets of distinct picolyl signals. The characteristic aldimine signals of **4a** and **4b** were observed at 9.17 and 9.08 ppm, respectively. Interestingly, when the measurements were carried out in DMSO-d_6, both **3a/4a** and **3b/4b** ratios were increased to 74/26 and 55/45, respectively (Table S3†).

Since preliminary results showed that aminals **3a** and **3b** exhibit dynamic covalent properties in solution, we further examined how the reaction is responsive to the environmental stimuli.

(a) Solvent effect. The equilibrium constants of **3a/4a** and **3b/4b** in various solvents were determined to evaluate the dynamic
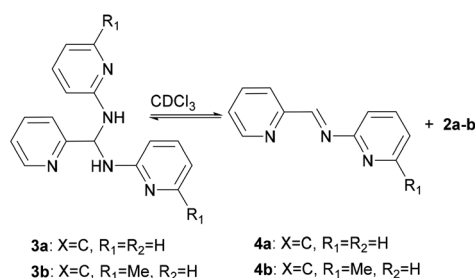
covalent properties for **3a** and **3b**. The equilibrium constant K_{eq} is defined as eqn (1):

$$K_{eq} = \frac{[\text{aminal}]}{[\text{imine}][\text{amine}]} \tag{1}$$

Various ratios of **2a/3a** or **2b/3b** respectively dissolved in CDCl₃, acetone-d_6, CD₃CN and DMSO-d_6 were prepared and monitored by ¹H NMR spectroscopy at 301 K using 1,3,5-trimethyl-2,4,6-trinitrobenzene as the internal standard. The K_{eq} values listed in Table 2 were obtained by a plot of [aminal] *vs.* [imine][amine] (Fig. S14–S21†). The results reveal that the formation of aminal is generally favoured in the more polar environment. In both cases, K_{eq} values derived from the DMSO-d_6 ($\varepsilon = 47.8$) and CD₃CN ($\varepsilon = 37.5$) systems are larger than that from CDCl₃ ($\varepsilon = 4.7$). The more polar environment would make the carbon on the imine group more electrophilic. As a result, nucleophiles such as amines attack the imine group more easily, increasing the yields of aminals. Quite the opposite, the more electron-donating amino moiety of **4b** would push electron density toward the electrophilic carbon atom and stabilize the imine group. Indeed, a comparison between the two systems shows that **3b**, the more electron-donating aminal, has a greater tendency to shift the equilibrium to imine.

To understand whether aminals **3c** and **3d** exhibit dynamic covalent properties or not, we examined their solution behaviours by NMR in six different solvents (listed in the order from lowest to highest dielectric constant: CDCl₃, pyridine-d_5 ($\varepsilon = 12.4$), acetone-d_6, CD₃NO₂ ($\varepsilon = 35.9$), CD₃CN and DMSO-d_6). Although the *N*-pyrimidyl substituted imines **4c** and **4d** cannot be detected in CDCl₃, pyridine-d_5 and DMSO-d_6, small amounts of them can be observed in acetone-d_6, CD₃NO₂ and CD₃CN. The aminal/imine ratios of **3c/4c** and **3d/4d** were found as 96/4 and 97/3 in acetone-d_6, 95/5 and 90/10 in CD₃NO₂, and 90/10 and 84/16 in CD₃CN (Table S3†). The less yields of **4c** and **4d** can be attributed to the more electron withdrawing pyrimidyl substituent on the N atom, leading to the formation of the more reactive C=N group easily attacked by a nucleophile.

C=N group stabilized by the n → π* interaction

Since the aminal/imine ratio depends on the reactivity of the C=N group, aminal forms should be more favoured in the more polar solvents. However, the result does not follow the order of the solvent polarity. We wondered the non-covalent intermolecular forces such as n → π* or π → π* interaction generated from the overlapping of the n or π orbital (from the solvent) and

Scheme 2 Equilibrating states for **3a** and **3b** in CDCl₃.

Table 2 Equilibrium constants of **3a/4a** and **3b/4b** in different solvents at 301 K

d-solvent	Dielectric constant (ε)	K_{eq} for **3a/4a**	K_{eq} for **3b/4b**
CDCl₃	4.81	31.70 ± 0.49	22.87 ± 0.46
Acetone-d_6	20.7	56.21 ± 0.13	32.05 ± 0.25
CD₃CN	37.5	63.38 ± 0.75	40.14 ± 0.74
DMSO-d_6	46.7	88.42 ± 0.40	38.06 ± 0.57

the π^* orbital (from the C=N group) would play a role in stabilizing the imine structures **4c** and **4d**.[49–54] Therefore, using **4c** system as a model, the density functional theory (DFT) calculation was performed to study the interactions between solvent molecules and imine **4c**. The equilibrium structures and the corresponding natural bonding orbital (NBO) analysis were carried out at the M06-2X-D3/def2TZVP level, and polarizable continuum model (PCM) was employed to simulate the solvation effect. The computing results reveal the C=N group of **4c** has the n → π^* interaction with CH_3CN, CH_3NO_2, acetone and CH_3OH but not $CHCl_3$, pyridine, and DMSO. As shown in Fig. 1 and Table 3, the solvent molecules of CH_3CN, CH_3NO_2, acetone and CH_3OH approach the C=N group on **4c** along the Bürgi-Duntiz (BD) trajectory.[50] All of them have the BD angles in the range of $107 \pm 10°$, and the distances between the donor atoms (O or N of the solvent molecules) and C=N are all smaller than the sum of their van der Waals radii. Besides, NBO analysis showed that the second order perturbation energies of MeOH, CH_3CN, CH_3NO_2 and acetone are respectively 2.22, 0.83, 0.69, and 0.35 kcal mol^{-1}, indicating the interaction between solvent molecule and $C=N_{4c}$ follows the order of MeOH $\gg$ CH_3CN > CH_3NO_2 > acetone. On the other hand, the distance of O on DMSO and C=N of **4c** is larger than 3.22 Å (the sum of the van der Waals radii for O and C), and the corresponding angle O–C–N was computed as 138.8°. Similarly, the interatomic distance between Cl_{CHCl3} and C=N of **4c** (3.54 Å) is longer than

Table 3 The geometrical parameters for Bürgi–Duntiz trajectory of solvent-**4c** dimers

Molecule pair	d (Å)	α (°)	$E_{n \to \pi*}$ (kcal mol^{-1})
Acetone-**4c**	3.027	108.9	0.35
CH_3CN-**4c-A**	3.228	115.8	0.83
CH_3NO_2-**4c**	3.148	115.5	0.69
CH_3OH-**4c**	2.944	99.1	2.22
DMSO-**4c**	3.374	138.8	0.09
$CHCl_3$-**4c**	3.540	118.1	0.13

the sum of their van der Waals radii (3.45 Å). The facts show there is no n → π^* non-covalent interaction between DMSO/$CHCl_3$ and **4c**. In the pyridine-**4c** case, the optimized structure showed the pyridine solvent molecule is parallel to imine group and fails to generate n → π^* non-covalent interaction with **4c** because of the improper orientation of the lone pair orbital of N. Instead, the second order perturbation energy analysis indicated that the π → π^* interaction exhibits in the parallel moieties of pyridine molecule and **4c**. However, the π → π^* interaction in the pyridine-**4c** system is smaller than that in the acetone-**4c** one (Fig. 2; 2nd perturbation energy in pyridine-**4c**: 0.22; acetone-**4c**: 0.37 kcal mol^{-1}). The optimized structure of CH_3CN-**4c** that the π orbitals of CH_3CN and **4c** were arranged in a parallel fashion, denoted as CH_3CN-**4c-B**, can be also obtained. CH_3CN-**4c-B** is 2.74 kcal mol^{-1} more stable than CH_3CN-**4c-A**, which has a CH_3CN fragment approaching C=N group of **4c** along the BD trajectory. The π → π^* interaction energy of CH_3CN-**4c-B** is calculated as 0.79 kcal mol^{-1}, higher than those of pyridine-**4c** and acetone-**4c**. No π → π^* interaction was found in both cases of CH_3NO_2-**4c** and DMSO-**4c**. Taken all together, **4c** can be observed in the CD_3CN, CD_3NO_2, and acetone-d_6 environments, all of which exhibit n → π^* interactions with **4c**. Among these solvents, no π → π^* interaction involves in the CD_3NO_2-**4c** dimer. In addition, **4c** cannot be observed in pyridine-d_5 although the π → π^* interactions are present in the pyridine-**4c** dimer. Therefore, we would suggest that the n → π^* non-covalent interaction contributes much more significantly to stabilize imine **4c** than the π → π^* one.

Detection of hemiaminal ethers in CD$_3$OD

Since the DFT calculation showed that the n → π^* interaction between the methanol molecule and the C=N group of **4c** is

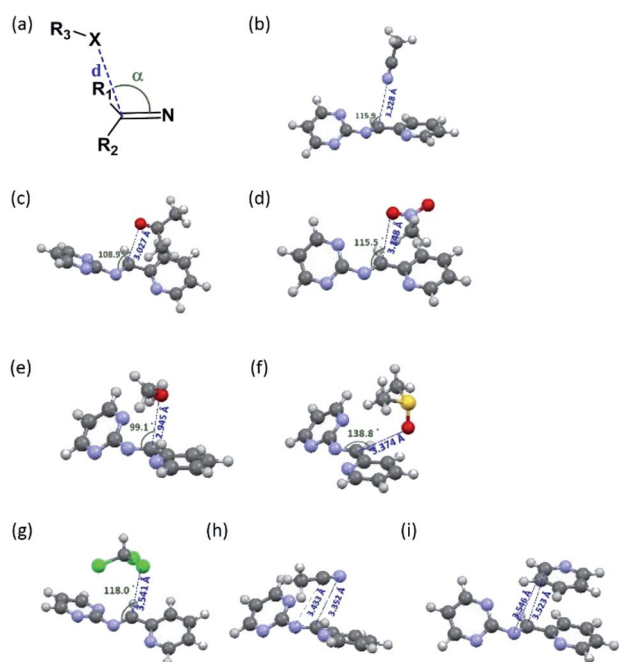**Fig. 1** (a) The structural parameters that characterize the n → π^* interaction. (b)–(i) DFT-optimized structures of solvent-**4c** dimers and their non-covalent interactions: (b) CH_3CN-**4c-A**: n → π^* interaction; (c) acetone-**4c**: both n → π^* and π → π^* interactions; (d) CH_3NO_2-**4c**: n → π^* interaction; (e) CH_3OH-**4c**: n → π^* interaction; (f) DMSO-**4c**: none; (g) $CHCl_3$-**4c**: none; (h) CH_3CN-**4c-B**: π → π^* interaction; (i) pyridine-**4c**: π → π^* interaction. The colours of the atoms are as follows: gray for C; white for H; blue for N; red for O; green for Cl; yellow for S.
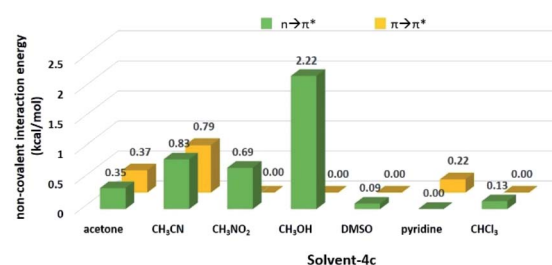

Fig. 2 The n → π^* and π → π^* interaction energy of solvent-**4c** dimers obtained from the DFT calculation.

high, we thus performed the NMR measurements of aminals **3a–d** in CD$_3$OD (sealed in a J-Young tube). As expected in what theoretical studies have suggested, only hemiaminal ethers **5a–d** and the corresponding amine signals were detected (Scheme 3). In cases of **3a** and **3b**, both show the disappearance of the imine singlet signals in the ^{1}H NMR spectra. Besides, each proton integration value for the heterocyclic amine moiety relative to the integration value of the methine proton is 1 : 1, suggesting the formation of the corresponding hemiaminal ethers **5a** and **5b**. The methine protons of **5a** and **5b** appeared at δ 6.20 and 6.09 ppm, respectively. In a like manner, for **5c** and **5d**, the proton peaks of methine CH and heterocyclic amine moiety showed the relative intensities 1 : 1. In each case, the ^{13}C NMR spectrum in CD$_3$OD showed a characteristic peak at around $\delta = 85$ ppm, which is assigned to the hemiaminal ether CH carbon and consistent with the literature.[55,56] On the other hand, the methine ^{13}C signals of aminals detected at around $\delta = 62$ ppm in CDCl$_3$ were absent when the measurements were carried out in CD$_3$OD. An attempt to isolate hemiaminal ethers has been failed since they were proceeded back to aminals under evaporation in all cases (Scheme 3).

Reaction of 3c and NaBH$_4$ in various solvents

Furthermore, we examined the reaction of **3c** and NaBH$_4$ in three different solvents. Neither methanol nor chloroform favour the existence of imine **4c**, and consequently no species can be reduced by NaBH$_4$. Only when conducting aforementioned reaction in acetonitrile under reflux, the corresponding amine **6c** can be obtained with a 33% yield (Scheme 4). The ^{1}H NMR spectrum of **6c** in CDCl$_3$ exhibits a singlet at $\delta = 4.75$ ppm, which is assigned to the picolylic protons. The structure was finally confirmed by the single crystal X-ray diffraction study. The ORTEP diagram of **6c** with 50% thermal ellipsoid probability is shown in Fig. 3, and the geometrical parameters are in consistent with the literature values.[57]

(b) Temperature effect. To understand the dynamic covalent bond strengths of aminals **3a–d**, we applied the linear van't Hoff plots to evaluate the thermodynamic parameters. The results of van't Hoff analysis shown in Table 4 are according to the variable temperature ^{1}H NMR spectra of **3a–d** in DMSO-d_6 recorded from 301 to 403 K. Herein, we define the equilibrium quotient (K_{eq}) as eqn (1). In each case, raising up the temperature causes the equilibrium to shift from the aminal side toward
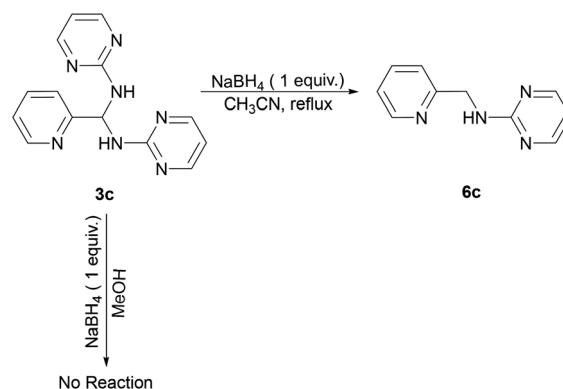
Scheme 4 Synthetic route for **6c**.

the imine side. As shown in Fig. 4(a) and (b), the yields of **3a** and **3b** are less than 10% when measuring at 388 K. After returning to room temperature, the 74/26 and 55/45 ratios for **3a/4a** and **3b/4b** reappeared. The fact implies that converting imine to aminal is a reversible and exothermic process, conforming to the negative changes in both enthalpy and entropy (ΔH and ΔS). The negative signs of ΔS in all cases support the fact that formation of aminal is the reaction combining two molecules to one. The differences of enthalpies for **3a** and **3b** are much smaller than those for **3c** and **3d**, indicating the breaking and formation of C–N bonds in **3a** and **3b** are more sensitive to the temperature stimulus. On the contrary, the N-pyrimidyl amino aminal systems have bond enthalpies above 150 kJ mol^{-1}, and **4c** cannot be even observed until heating up to 378 K.

(c) Acidic and basic influence. Next, we used **3b** as a model to inspect the equilibrium change with the presence of different amounts of acid and base. As Fig. S28 and S29† have shown, the spectra undergo no change in base media (from 0 to 2.4 equivalent of triethylamine). However, the equilibrium of **3b/4b** is very sensitive in an acid medium. The ratio of **3b/4b** decreases from 1.5 to 0.7 with the presence of 0 to 0.85 equiv. of acetic acid in CDCl$_3$. This observation suggests that aminals such as **3b**, are fairly stable in the basic condition and easily undergo deamination in the acidic condition. On the other hand, addition of acetic acid easily gives rise to the decomposition of **3b** and **4b**. In Fig. S29,† the proton signal of 2-pyridinecarboxaldehyde has been observed at 8.77 ppm. The peak intensity increases with the increases of the amounts of acetic acid. The breakdown of **3b** and **4b** is attributed to the protonation of the amine group in the acidic condition, leading to the formation of iminium
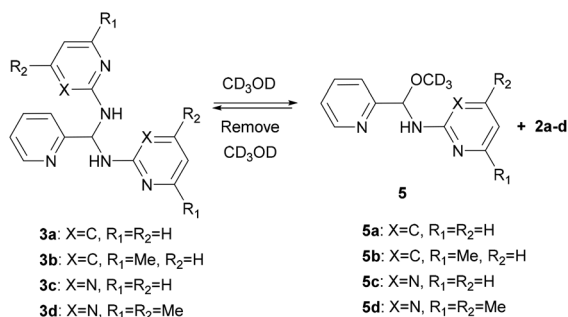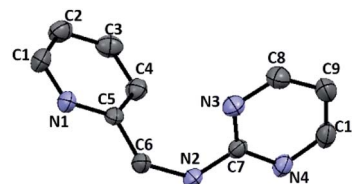
Scheme 3 Formation of **5a–d**.

Fig. 3 ORTEP drawing of **6c** with 50% probability thermal ellipsoids. Hydrogen atoms are omitted for clarity. Selected distances (Å) and angles (deg.): C6–N2 1.4468(15), N6–C6–C5 114.39(10).

Table 4 Thermodynamic parameters of aminals **3a–d** in DMSO-d_6 derived from van't Hoff equation[a]

| Aminal	ΔH (kJ mol^{-1})	ΔS (J mol^{-1} K^{-1})
3a	-53.56 ± 1.36	-2.05 ± 0.06
3b	-32.41 ± 0.70	-1.13 ± 0.03
3c[b]	-173.58 ± 9.44	-4.58 ± 0.12
3d[c]	-155.31 ± 7.08	-5.14 ± 0.27

[a] Initial concentration used: 0.070 mmol of **3a**; 0.036 mmol of **3b**; 0.037 mmol of **3c**; 0.0310 mmol of **3d** was dissolved in 0.5 mL of DMSO-d_6. [b] Derived from $T = 378$ to 403 K. [c] Derived from $T = 358$ to 403 K.

cation and the release of amine. Subsequently, the iminium ion is subject to conventional hydrolysis at the presence of water in acetic acid.

A strategy for the synthesis of a picolyl aromatic amino aminal

Learning from the synthesis of the picolyl heterocyclic amino aminal, we were therefore tempted to synthesize a picolyl aromatic amino aminal from an electron withdrawing aromatic amines. **3e** was successfully obtained by mixing 1 equivalent of 2-pyridinecarboxaldehyde with 2 equivalent of 2-methoxy-5-nitroaniline in methanol at room temperature in 86.4% yield. The solid state structure of **3e** is confirmed by the single crystal X-ray diffraction shown in Fig. 5. **3e** also exhibits a dynamic covalent property in solution. Similar to the cases of picolyl heterocyclic amino analogues, the ratios of aminal (**3e**)/imine (**4e**) in CDCl$_3$ and DMSO-d_6 are respectively 11/89 and 20/80 at room temperature (initial concentrations of **3e**: 5.0/0.5 mg mL^{-1} in

CDCl$_3$; 16.3/0.6 mg mL^{-1} in DMSO-d_6). Variable-temperature ^{1}H NMR (DMSO-d_6) shows that **3e** totally converts to **4e** above 373 K. The thermodynamic parameters derived from 301, 343, 373 and 403 K were calculated as $\Delta H = -38.44 \pm 2.36$ kJ mol^{-1} and $\Delta S = -1.65 \pm 0.10$ J mol^{-1} K^{-1}. On the other hand, when the measurement is carried out in CD$_3$OD, only hemiaminal **5e** and 2-methoxy-5-nitroaniline can be detected (Scheme 5).
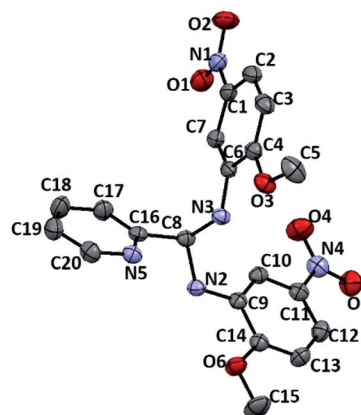

Fig. 5 ORTEP drawing of **3e** with 50% probability thermal ellipsoids. Hydrogen atoms are omitted for clarity. Selected distances (Å) and angles (deg.): C8–N3 1.449(2), C8–N2 1.457(2), C1–N5 1.460(3), C11–N4 1.454(3), N5–O6 1.229(2), N5–O5 1.233(2), N4–O4 1.229(2), N4–O3 1.233(2), C14–O1 1.361(2), C15–O1 1.431(3), C4–O2 1.357(2), C5–O2 1.428(3), N3–C8–N2 109.63(15), O6–N5–O5 123.0(2), O4–N4–O4 122.24(18), C4–O2–C5 118.66(17), C14–O1–C15 117.57(17).
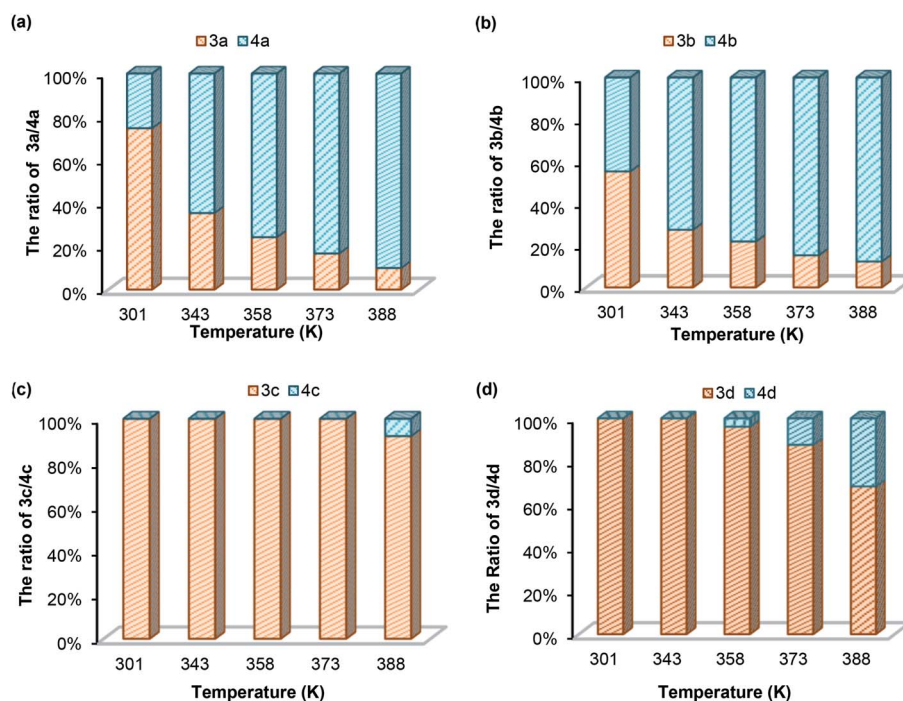
Fig. 4 Aminal/imine ratios for (a) **3a/4a**; (b) **3b/4b**; (c) **3c/4c**; (d) **3d/4d** in DMSO-d$_6$ at different temperatures.
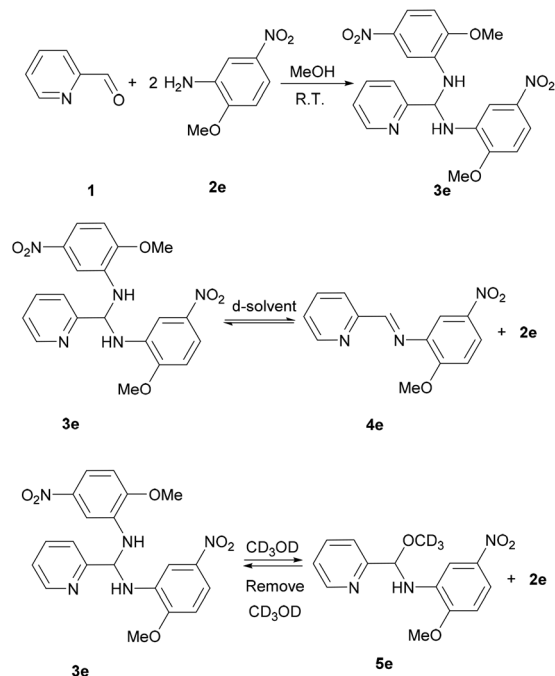
Scheme 5 Synthesis and dynamic covalent properties for **3e**.

Conclusions

In summary, synthesis of a series of the picolyl heterocyclic amino aminals and the characterization of their dynamic covalent properties have been reported in this work. The formation and breakdown of the aminal bond is very dependent on the solvent, the acid/base, the temperature, and the natures of the amines. The heterocyclic amine is more electron-withdrawing than aniline, making the corresponding imine more polar and easily be attacked by a nucleophile. As a result, the essence of the amine as well as the intermolecular force that can prevent C=N group from nucleophilic addition play crucial roles to shift the equilibrium to imine side. Although the polar solvent facilitates amine to attack imine and affords more aminal forms, the lone pair on the solvent may stabilize the C=N group of imine *via* n → π* interaction. Accordingly, acetonitrile presents a higher preference toward imine forms. Moreover, aminals **3a–d** totally convert to hemiaminal ethers **5a–d** in methanol, supporting the DFT calculation result of the strongest n → π* interaction between methanol and imine **4c**. According to these natures, **6c** can be obtained from reduction of **3c** by $NaBH_4$ in acetonitrile but not in methanol. We also succeeded in the synthesis of a novel picolyl aromatic amino aminal **3e** by using the electron-withdrawing 2-methoxy-5-nitroaniline as the starting material. After examining the physical organic properties of **3e**, we also confirmed **3e** exhibits a dynamic aminal bond and would give different responses with the different environmental stimuli.

Conflicts of interest

There are no conflicts to declare.

Notes and references

1 A. Herrmann, *Chem. Soc. Rev.*, 2014, **43**, 1899–1933.
2 Y. Jin, C. Yu, R. J. Denman and W. Zhang, *Chem. Soc. Rev.*, 2013, **42**, 6634–6654.
3 J.-M. Lehn, *Angew. Chem., Int. Ed.*, 2013, **52**, 2836–2850.
4 K. Meguellati and S. Ladame, in *Constitutional Dynamic Chemistry*, ed. M. Barboiu, Springer Berlin Heidelberg, Berlin, Heidelberg, 2012, pp. 291–314, DOI: 10.1007/128_2011_277.
5 S. J. Rowan, S. J. Cantrill, G. R. L. Cousins, J. K. M. Sanders and J. F. Stoddart, *Angew. Chem., Int. Ed.*, 2002, **41**, 898–952.
6 P. T. Corbett, J. Leclaire, L. Vial, K. R. West, J.-L. Wietor, J. K. M. Sanders and S. Otto, *Chem. Rev.*, 2006, **106**, 3652–3711.
7 F. Schaufelberger, B. Timmer and O. Ramström, in *Dynamic Covalent Chemistry*, ed. W. Zhang and Y. Jin, John Wiley & Sons, New York City, USA, 2017, pp. 1–30, DOI: 10.1002/9781119075738.ch1.
8 Y. Zhang, S. Xie, M. Yan and O. Ramström, *Chem.–Eur. J.*, 2017, **23**, 11908–11912.
9 S. Ladame, *Org. Biomol. Chem.*, 2008, **6**, 219–226.
10 J.-M. Lehn, *Chem.–Eur. J.*, 1999, **5**, 2455–2463.
11 C.-W. Hsu and O. Š. Miljanić, *Angew. Chem., Int. Ed.*, 2015, **54**, 2219–2222.
12 J.-M. Lehn, *Chem. Soc. Rev.*, 2007, **36**, 151–160.
13 G. Vantomme, S. Jiang and J.-M. Lehn, *J. Am. Chem. Soc.*, 2014, **136**, 9509–9518.
14 H. Zheng, C. Ni, H. Chen, D. Zha, Y. Hai, H. Ye and L. You, *ACS Omega*, 2019, **4**, 10273–10278.
15 D. Komáromy, M. C. A. Stuart, G. Monreal Santiago, M. Tezcan, V. V. Krasnikov and S. Otto, *J. Am. Chem. Soc.*, 2017, **139**, 6234–6241.
16 V. E. Campbell, X. de Hatten, N. Delsuc, B. Kauffmann, I. Huc and J. R. Nitschke, *Nat. Chem.*, 2010, **2**, 684–687.
17 M. N. Chaur, D. Collado and J.-M. Lehn, *Chem.–Eur. J.*, 2011, **17**, 248–258.
18 R. Göstl and S. Hecht, *Angew. Chem., Int. Ed.*, 2014, **53**, 8784–8787.
19 J. Holub, G. Vantomme and J.-M. Lehn, *J. Am. Chem. Soc.*, 2016, **138**, 11783–11791.
20 G. Nicolas, F. Gad and J.-M. Lehn, *Chem.–Eur. J.*, 2006, **12**, 1723–1735.
21 Y. Hai, H. Zou, H. Ye and L. You, *J. Org. Chem.*, 2018, **83**, 9858–9869.
22 P. J. Boul, D. Rasner and C. J. Thaemlitz, *Ind. Eng. Chem. Res.*, 2018, **57**, 17043–17047.

23 D. E. Apostolides and C. S. Patrickios, *Polym. Int.*, 2018, **67**, 627–649.

24 Y. Tao, S. Liu, Y. Zhang, Z. Chi and J. Xu, *Polym. Chem.*, 2018, **9**, 878–884.

25 Y. Zhang, C.-Y. Pham, R. Yu, E. Petit, S. Li and M. Barboiu, *Front. Chem.*, 2020, **8**, 739, DOI: 10.3389/fchem.2020.00739.

26 K. Fukuda, M. Shimoda, M. Sukegawa, T. Nobori and J.-M. Lehn, *Green Chem.*, 2012, **14**, 2907–2911.

27 M. E. Belowich and J. F. Stoddart, *Chem. Soc. Rev.*, 2012, **41**, 2003–2024.

28 M. Ciaccia, R. Cacciapaglia, P. Mencarelli, L. Mandolini and S. Di Stefano, *Chem. Sci.*, 2013, **4**, 2253–2261.

29 M. Ciaccia and S. Di Stefano, *Org. Biomol. Chem.*, 2015, **13**, 646–654.

30 S. Kulchat, M. N. Chaur and J.-M. Lehn, *Chem.–Eur. J.*, 2017, **23**, 11108–11118.

31 J. K. Laha, K. S. S. Tummalapalli and K. P. Jethava, *Org. Biomol. Chem.*, 2016, **14**, 2473–2479.

32 A. Chao, I. Negulescu and D. Zhang, *Macromolecules*, 2016, **49**, 6277–6284.

33 Y. Jin, Q. Wang, P. Taynton and W. Zhang, *Acc. Chem. Res.*, 2014, **47**, 1575–1586.

34 G. K. Cantrell and T. Y. Meyer, *Organometallics*, 1997, **16**, 5381–5383.

35 A. G. Tennyson, B. Norris and C. W. Bielawski, *Macromolecules*, 2010, **43**, 6923–6935.

36 Y. Zhou, L. Li, H. Ye, L. Zhang and L. You, *J. Am. Chem. Soc.*, 2016, **138**, 381–389.

37 Y. Zhou, Y. Yuan, L. You and E. V. Anslyn, *Chem.–Eur. J.*, 2015, **21**, 8207–8213.

38 L. Artús Suàrez, Z. Culakova, D. Balcells, W. H. Bernskoetter, O. Eisenstein, K. I. Goldberg, N. Hazari, M. Tilset and A. Nova, *ACS Catal.*, 2018, **8**, 8751–8762.

39 Á. Beltrán, E. Álvarez, M. M. Díaz-Requejo and P. J. Pérez, *Adv. Synth. Catal.*, 2015, **357**, 2821–2826.

40 A. Castro-Alvarez, H. Carneros, D. Sánchez and J. Vilarrasa, *J. Org. Chem.*, 2015, **80**, 11977–11985.

41 Y.-H. Chen, X.-J. Lv, Z.-H. You and Y.-K. Liu, *Org. Chem. Front.*, 2019, **6**, 3725–3730.

42 Y.-Y. Huang, C. Cai, X. Yang, Z.-C. Lv and U. Schneider, *ACS Catal.*, 2016, **6**, 5747–5763.

43 M. Islam, M. Razzak, M. Karim and A. H. Mirza, *Tetrahedron Lett.*, 2017, **58**, 1429–1432.

44 U. Orcel and J. Waser, *Angew. Chem., Int. Ed.*, 2016, **55**, 12881–12885.

45 B. Buchs, G. Godin, A. Trachsel, J.-Y. de Saint Laumer, J.-M. Lehn and A. Herrmann, *Eur. J. Org. Chem.*, 2011, **2011**, 681–695.

46 J. Tessarolo, A. Venzo, G. Bottaro, L. Armelao and M. Rancan, *Eur. J. Inorg. Chem.*, 2017, **2017**, 30–34.

47 I. Iovel, L. Golomba, J. Popelis, S. Grinberga, S. Belyakov and E. Lukevics, *Chem. Heterocycl. Compd.*, 2002, **38**, 1210–1229.

48 H. L. Zhu, Q. X. Liu, A. Usman and H. K. Fun, *Z. Kristallogr. N. Cryst. Struct.*, 2003, **218**, 317.

49 A. J. Neel, M. J. Hilton, M. S. Sigman and F. D. Toste, *Nature*, 2017, **543**, 637–646.

50 R. W. Newberry and R. T. Raines, *Acc. Chem. Res.*, 2017, **50**, 1838–1846.

51 V. Angarov and S. Kozuch, *New J. Chem.*, 2018, **42**, 1413–1422.

52 B. Sahariah and B. K. Sarma, *Chem. Sci.*, 2019, **10**, 909–917.

53 K. B. Muchowska, D. J. Pascoe, S. Borsley, I. V. Smolyar, I. K. Mati, C. Adam, G. S. Nichol, K. B. Ling and S. L. Cockroft, *Angew. Chem., Int. Ed.*, 2020, **59**, 14602–14608.

54 H. Chen, H. Ye, Y. Hai, L. Zhang and L. You, *Chem. Sci.*, 2020, **11**, 2707–2715.

55 R. El Mail, M. A. Garralda, R. Hernández, L. Ibarlucea, E. Pinilla and M. R. Torres, *Organometallics*, 2000, **19**, 5310–5317.

56 M. A. Garralda, R. Hernández, L. Ibarlucea, E. Pinilla, M. R. Torres and M. Zarandona, *Organometallics*, 2007, **26**, 5369–5376.

57 S.-H. Moon, T. H. Kim and K.-M. Park, *Acta Crystallogr., Sect. E: Struct. Rep. Online*, 2011, **67**, o1355.